Synthesis and Characterization of Conjugated Diblock Copolymers

Hengbin Wang,[a] Man-Kit Ng,[a] Liming Wang,[a] Luping Yu,*[a] Binhua Lin,[b] Mati Meron,[b] and Yanan Xiao[b]

Abstract: This paper reports the synthesis and characterization of a new class of diblock copolymers (co-oligomers), rod–rod conjugated diblock copolymers. A general synthetic strategy is outlined, and the structures of the copolymers (oligothiophene–*co*-oligophenylenevinylene) are fully characterized. It was found that these copolymers exhibit efficient intramolecular energy transfer. An interesting self-assembly ability of these rod–-rod copolymers was also revealed.

Keywords: block copolymers · conjugation · energy transfer · phase separation

Introduction

The extended π-electronic systems of conjugated polymers give the materials numerous physical properties, which resemble those of a typical inorganic semiconductor. Properties such as high electric conductivity after chemical doping, optical nonlinearity, and electroluminescence have been demonstrated in the past decades.[1–3] These materials offer scientists an opportunity to explore new and different concepts in solid-state devices, such as organic light-emitting diodes,[4] field effect transistors, chemical sensors, and all-polymeric optic-electronic devices.

More recently, interest has grown in organizing these materials into three-dimensional structures so that novel morphologies, and even new properties can be observed, and a better understanding of the property–structure relationship can be obtained. A typical example is the synthesis and study of rod–coil types of diblock copolymers, in which one of the blocks is a conjugated block.[5–7] Interesting morphologies including spherical, cylindrical, and lamella nanometer structures have been observed. However, an important class of block copolymers, rod–rod conjugated diblock copolymers, has not been reported in the literature probably due to the synthetic difficulty. A conjugated diblock copolymer will certainly behave differently from rod–coil types of structures. A fundamental question is what kind of electronic and structural properties will these rod–rod types of diblock copolymers exhibit. These systems offer the opportunity to explore an unknown domain that could be fruitful for discovering new knowledge and generating new materials. This paper reports our recent successful efforts in synthesizing several conjugated diblock polymers (or oligomers) and their physical and morphological studies.

[a] Prof. Dr. L. Yu, H. Wang, M.-K. Ng, Dr. L. Wang
5735 South Ellis Avenue
Department of Chemistry and James Franck Institute
The University of Chicago, Chicago, IL 60637 (USA)
Fax: (+1) 773-702-0805
E-mail: lupingyu@midway.uchicago.edu

[b] Dr. B. Lin, Dr. M. Meron, Dr. Y. Xiao
Center for Advanced Radiation Sources and James Frank Institute
University of Chicago, 5640 South Ellis Avenue
Chicago, IL 60637 (USA)

Results and Discussion

Synthesis and structural characterization: Scheme 1 shows the synthetic approach of these copolymers (Copolymers **5a–c**). In this scheme, two conjugated blocks were prepared in a stepwise synthetic approach developed in our laboratory.[5, 10, 11] There are several reasons for selecting oligo(phenylenevinylene) (OPV) and oligothiophene (OT) as the two blocks. Firstly, both oligo(phenylenevinylene) and oligothiophene possess very interesting optical and electronic properties.[1–4] Secondly, all-*trans* oligo(phenylenevinylenes) are very rigid molecules exhibiting liquid crystallinity; oligoalkylthiophene is completely amorphous when the alkyl groups on the 3-position of the thiophene repeating units are racemic, β-branched side chains. A significant difference in χ values between the two blocks can thus be expected. For example, the solubility parameters for various polymer repeating units present in the diblock copolymers can be estimated by group contribution methods developed by Van Krevelen.[12] The calculated values are: oligo(3-hexylthiophene) 18.7 $J^{1/2}/cm^{3/2}$; oligo(alkyl-substituted phenylenevinylene) 19.6 $J^{1/2}/cm^{3/2}$. Finally, the structures of both blocks can be modified with electron-rich or -deficient substituents. A methyl ester group was attached to the oligothiophene block to increase the polarity of the copolymers so as to facilitate the purification of the final products. It was found that compound **1a** could not

  0947-6539/02/0814-3246 $ 20.00+.50/0

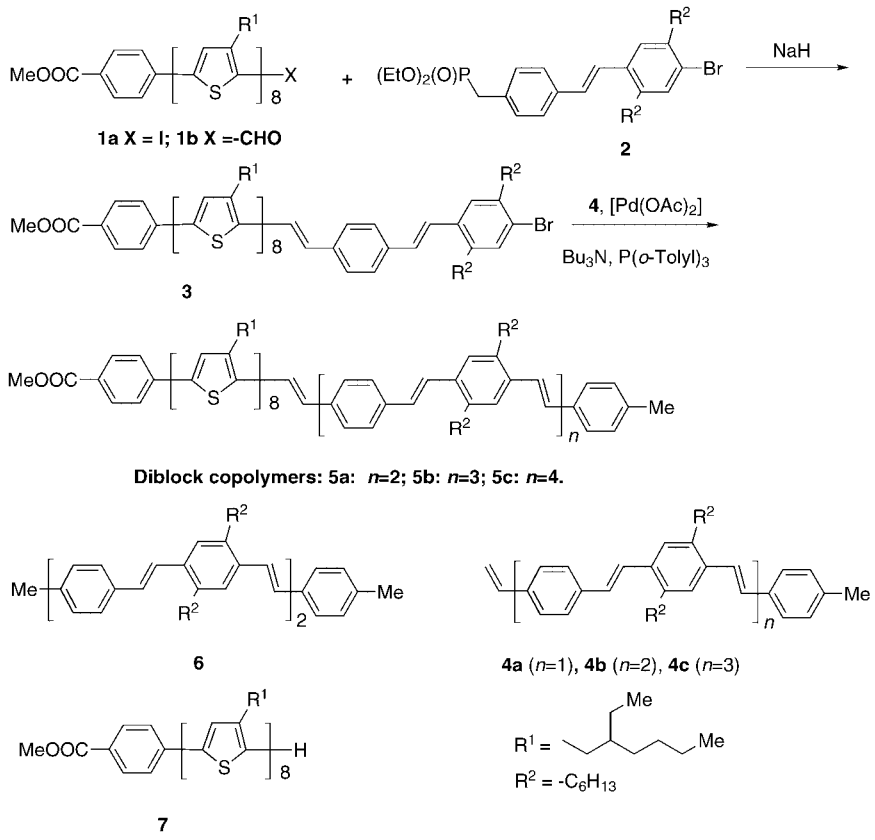

Scheme 1. Synthesis of conjugated diblock copolymers.

undergo the coupling reaction with compound **4** under the normal Heck reaction conditions. Compound **3** was thus synthesized from corresponding compounds **1b** and **2**. The Heck coupling between compounds **4** and **3** went smoothly and generated diblock copolymers with good yields. The final products were purified by column chromatography (silica gel) using ethyl acetate/hexane or a chloroform/hexane mixture as the eluent.

All three copolymers are very soluble in chloroform or THF, copolymer **5a** is very soluble in hexane, **5b** is less so, and **5c** is almost completely insoluble in hexane. Each of these copolymers possesses a single molecular weight as shown by a single sharp peak from the GPC spectrum (polydispersity ≈ 1). The elemental analyses were consistent with the copolymer composition, and matrix-assisted laser desorption ionization (MALDI) mass spectra of these compounds showed molecular weights of copolymers **5a** (2551.57), **5b** (2923.99), and **5c** (3299.55).

The chemical structures of these copolymers were confirmed by ^{1}H and ^{13}C NMR spectroscopy. All of the chemical shifts corresponding to the oligo(phenylenevinylene) and oligothiophene blocks appear in the ^{1}H and ^{13}C NMR spectra.

Because these all-*trans*-OPVs are rigid molecules, all of the copolymers manifest a reversible thermotropic liquid-crystalline phase (LC). The LC–isotropic transition of three copolymers was clearly observed at 83.6, 144.2, and 189.1 °C for copolymers **5a**, **5b**, and **5c**, respectively, from DSC traces of heating scans with a scan rate of 10 °C min^{-1}. The reversed transition was observed at 58, 110, and 167 °C, respectively, from DSC traces of cooling scans. But the glass transition temperatures of the copolymers and the crystalline melting peaks corresponding to the OPV blocks were not observed. This is consistent with our previous studies of OPV–PEG block copolymers;[7] a visible crystalline melting peak of an OPV block can be observed only for an OPV with 13 or more phenyl rings. Polarized optical microscopic studies of these copolymers confirmed the LC–isotropic phase transition temperature.

Cyclic voltammetry studies revealed complicated features of the electrochemistry of these copolymers (Figure 1). Three oxidation processes (0.79, 1.03, and 1.32 V vs Ag^+/Ag) can be noted for compound **6**. The CV results for oligothiophene **7** indicated four oxidation processes at 0.54, 0.66, 1.02, and 1.19 V. As the chain length increases, overlapping of the redox waves complicates the determination of the oxidation potentials for the copolymers. The first and second oxidation potentials for copolymer **5a** were cathodically shifted to +0.50 and +0.59 V with respect to oligothiophene **7**. Three more oxidation potentials appeared at 0.74, 0.87, and 1.06 V. No reduction process was observed for all compounds within the range from 0 to −1.6 V versus Ag/Ag^+.

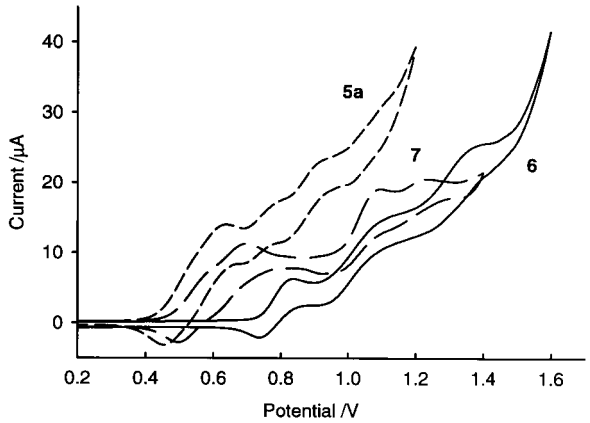

Figure 1. Cyclic voltammograms of compounds **6**, **7**, and copolymer **5a** in 0.1M $Bu_4N^+ClO_4^-/CH_2Cl_2$; scan rate 100 mV s^{-1}, reference Ag/Ag^+.

TEM studies: Although both blocks of these copolymers are hydrophobic rigid rods, TEM studies revealed an interesting self-assembling ability of these rod–rod copolymers. It was found that the compositions of the diblock copolymers affect the morphology of the resulting assembly significantly (Figure 2 **A**, **B**, and **C**). Copolymers **5a**, **5b**, and **5c** possess the

  0947-6539/02/0814-3247 $ 20.00+.50/0

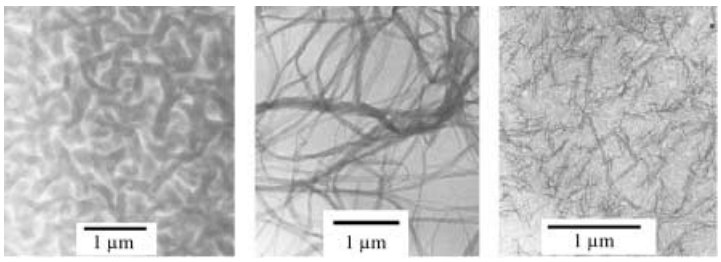

Figure 2. TEM images of films of copolymers **5a** (**A**), **5b** (**B**), and **5c** (**C**) prepared by placing a drop of the solution onto a carbon-coated copper grid or SiN grid. The grids were dried under a solvent atmosphere. The specimen was then examined by using a Philips CM 120 electron microscope operated at 120 kV.

same oligothiophene block but differ in the number of phenylenevinylene units. This small difference causes the morphology of copolymer films to change from an interwoven network (copolymer **5a**, **A**) to layered stripes (copolymer **5b**, **B**) and to lamella (copolymer **5c**, **C**) when the hexane/chloroform (10%) mixture was used as the solvent. Both carbon-coated copper grids and SiN grids were used as the substrate. No morphological change was observed after the samples were annealed at 100°C for 24 hours.

It was also found that the solvent used to prepare films affected the morphologies of these copolymers. When pure chloroform was used as the solvent, the morphology of copolymer **5b** changed to an interwoven network, and **5c** changed to layered stripes.

X-ray diffraction studies: SAXS studies were carried out to further identify the molecular packing for morphologies of these copolymers. Figure 3a shows the SAXS profiles of the

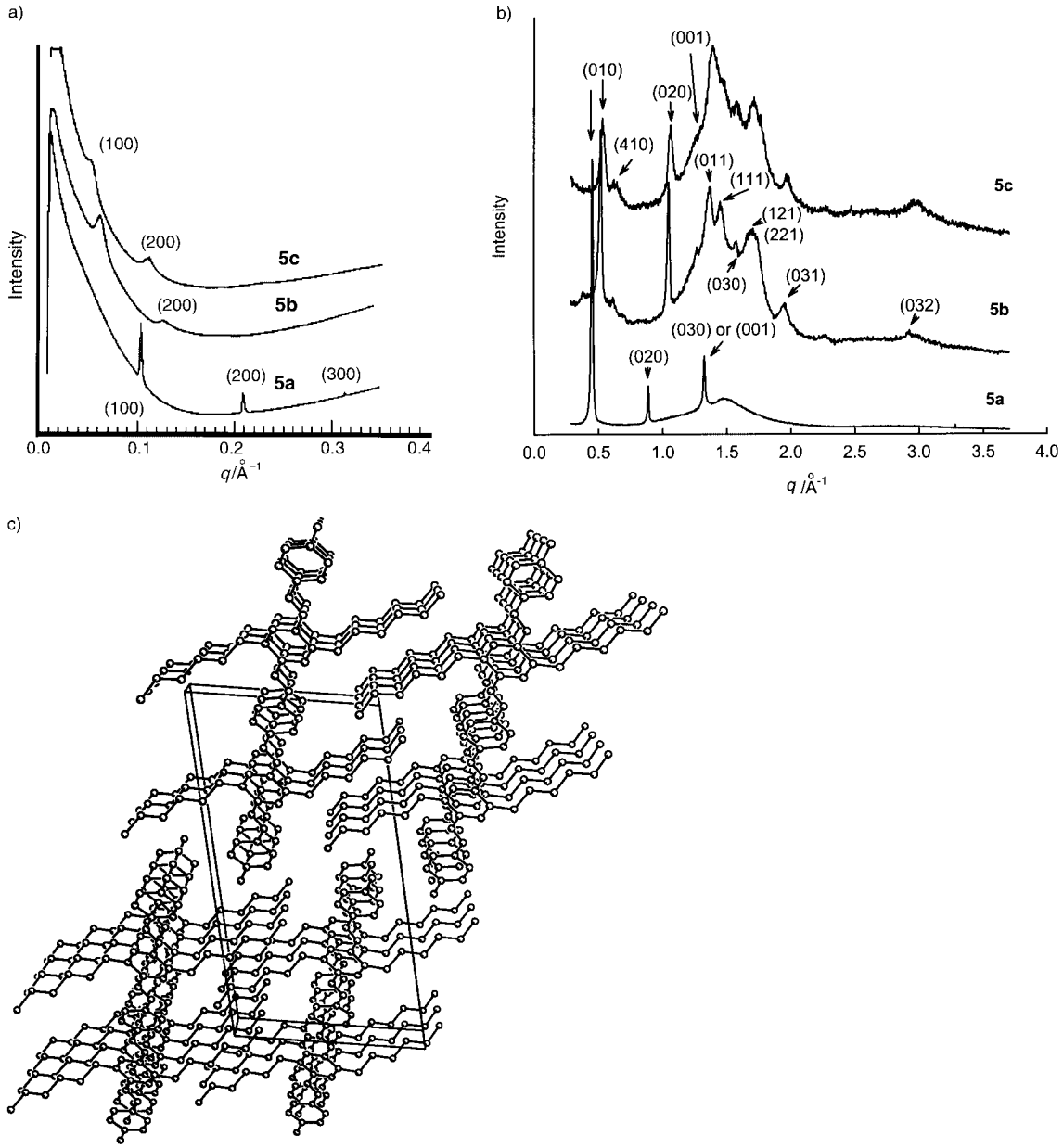

Figure 3. a) Small-angle X-ray scattering patterns of copolymers **5a**, **5b**, and **5c** at room temperature; b) wide-angle X-ray diffraction profiles of copolymers **5a**, **5b**, and **5c** at room temperature; c) schematic representation of the single-crystal packing structure of compound **6**.

0947-6539/02/0814-3248 $ 20.00+.50/0 *Chem. Eur. J.* **2002**, *8*, No. 14

three copolymers at room temperature. The diffraction patterns consist of two to three Bragg reflections with equal reciprocal spacing, which indicates a lamella microstructure. The calculated molecular lengths and the corresponding lamellar spacings are listed in Table 1. It can be noted that compound **5a** has a smaller spacing than the calculated one. The difference in measured spacing between **5a** and **5b** (4 nm) is much larger than that between **5b** and **5c** (1.5 nm),

Table 1. Structural parameters for the diblock copolymers **5a**, **5b**, and **5c**.

Copolymers	**5a**	**5b**	**5c**
calculated molecular length [nm][a]	6.8	8.1	9.4
measured layer spacing [nm][b]	6.0	10.0	11.5

[a] Results estimated from Chem-3D calculation. [b] SAXS results.

although the molecular structures differ just by two phenylenevinylene units (1.3 nm). These results indicate that the molecular packing in the lamella of compound **5a** is different from those of compounds **5b** and **5c**. To accommodate these results, we propose that compound **5a** forms lamella with a single molecular layer arrangement (Scheme 2a). The SAXS shows the diffractions from (100), (200), and (300) lattice planes with the lattice parameter of 6 nm. In this model, each molecule is tilted against the layer with an angle of 60°, which will give rise to a layered structure with a thickness of 6 nm. However, the SAXS results only indicate one-dimensional arrangements. Wide-angle X-ray diffraction studies must be used to identify the three-dimensional structure of the lamella. Since these molecules cannot form single crystals large enough for precise structural determination, annealed samples were used. The WAXD results for compound **5a** are very simple and are shown in Figure 3b. There are three sharp diffraction peaks in addition to a very diffused diffraction due to an amorphous phase. The assignments of these peaks are indicated in Figure 3b. The (010) and (020) diffractions can be assigned with confidence and they correspond to a lattice parameter of 1.400 nm. The diffraction at *d* spacing of 0.483 nm can be assigned to either (030) or (001) or both. Judging from the diffraction intensity change from (010) to (020), we can attribute this diffraction mainly to diffraction (001), corresponding to the interdistance between π-orbital planes. These assignments are consistent with the single-crystal structure of compound **6a**, which has a triclinic lattice structure (Figure 3c and Table 2).

Clearly, even the OPV5 lattice exhibits a layered structure. The *b* and *c* lattice parameters are very similar to those in co-oligomer **5a**, which is not unexpected. It can be explained based on the fact that the addition of an OT8 block increased the thickness of the layer with minimal perturbation to the lateral intermolecular distance. However, since Figure 3b shows no high order diffraction for **5a**, it is difficult to determine the exact lattice structure because the angular information cannot be obtained. The reason for the absence of the higher order diffraction could be due to the difficulty for the OT8 block to form a regular crystal lattice because the side chains of the OT8 are racemic alkyl groups. Another uncertainty is the interlayer registration. It is unknown whether the interlayer molecules are stacked together head-to-tail or there is a shift as shown in the crystal structure of **6** (Figure 3c). For co-oligomers **5b** and **5c**, their X-ray diffraction patterns are very similar. The SAXS results indicated layered structures with a larger spacing for **5c** than **5b**. However, the measured layer spacings of copolymer films **5b** and **5c** are larger than the calculated molecular lengths, so the lamella layer must consist of two molecules. Tentatively, we propose that two of the diblock molecules stick together head to head to form the repeating unit. This repeating unit is tilted with an angle of 38° against the layer planes for both **5b** and **5c** (Scheme 2b). The WAXD results of these two molecules are almost identical. They have higher order diffractions. A tentative assignment for several featured peaks based on **5a** and OPV5 results is indicated in Figure 3b. For **5b**, for example, the (010) diffraction has a *d* spacing of 1.21 nm. The (020) or even (030) peaks can be identified. The $\pi-\pi$ interplane distance of 0.491 nm can be identified. The higher order diffraction peaks can be assigned based on the parameters of $a=10.0$, $b=1.21$, and $c=0.493$ nm, and $\alpha=91$, $\beta=91$, and $\gamma=101°$. It has to be mentioned that these assignments are not conclusive, as the X-ray results for the polymeric materials will be due to the lack of single-crystal data, and the fact that many diffraction peaks are diffused. However, the lattice parameters deduced are self-consistent with all of the experimental facts.

Optical properties: The optical properties of the copolymers **5a–c** and simple oligo(phenylenevinylene) **6** and oligothiophene **7** were studied in solution in chloroform (4.8×10^{-7} M) by UV/Vis absorption spectroscopy (Figure 4) and emission spectroscopy (Figure 4). Broad and featureless absorption bands were observed in all the spectra and could be ascribed to the $\pi-\pi^*$ transition of the conjugated backbones. The absorption maxima of compounds **6** and **7** appear at 394 and 418 nm, respectively. After the oligo(phenylenevinylene) and oligothiophene were coupled, an electronic transition appears at 426 nm for copolymer **5a** due to the increase in conjugation length. No red shift was observed after a further increase in phenylenevinylene units in copolymer **5b** and **5c**, which indicated saturation of the electron delocalization. Photoemission of compound **6** excited at 400 nm produces a typical spectrum of alkyl-substituted oligo(phenylenevinylene) in solution: a strong fluorescence at 460 nm with two small shoulders at about 489 and 530 nm derived from low-energy vibronic side bands with a quantum efficiency of 79.9%. Compound **7** gives a weak and featureless emission band with an emission maximum at 564 nm with a quantum efficiency of 14.2%. Copolymers **5a**, **5b**, and **5c** give rise to almost exactly the same emission spectra as compound **7** with a quantum efficiency of 14.6, 14.5, and 14.8%, respectively. Emission from the phenylenevinylene units was completely quenched, implying a complete intramolecular energy transfer from the oligo(phenylenevinylene) block to the oligothiophene block. Similar behavior was observed for the other two copolymers. Figure 5 shows the combination of excitation and absorption spectra of copolymer **5a** plus the absorption spectra of compound **6**. When the emission wavelength was chosen to be the maximum emission of copolymer **5a** (540 nm), we see a complete overlap of peaks of the absorption spectrum of **5a**

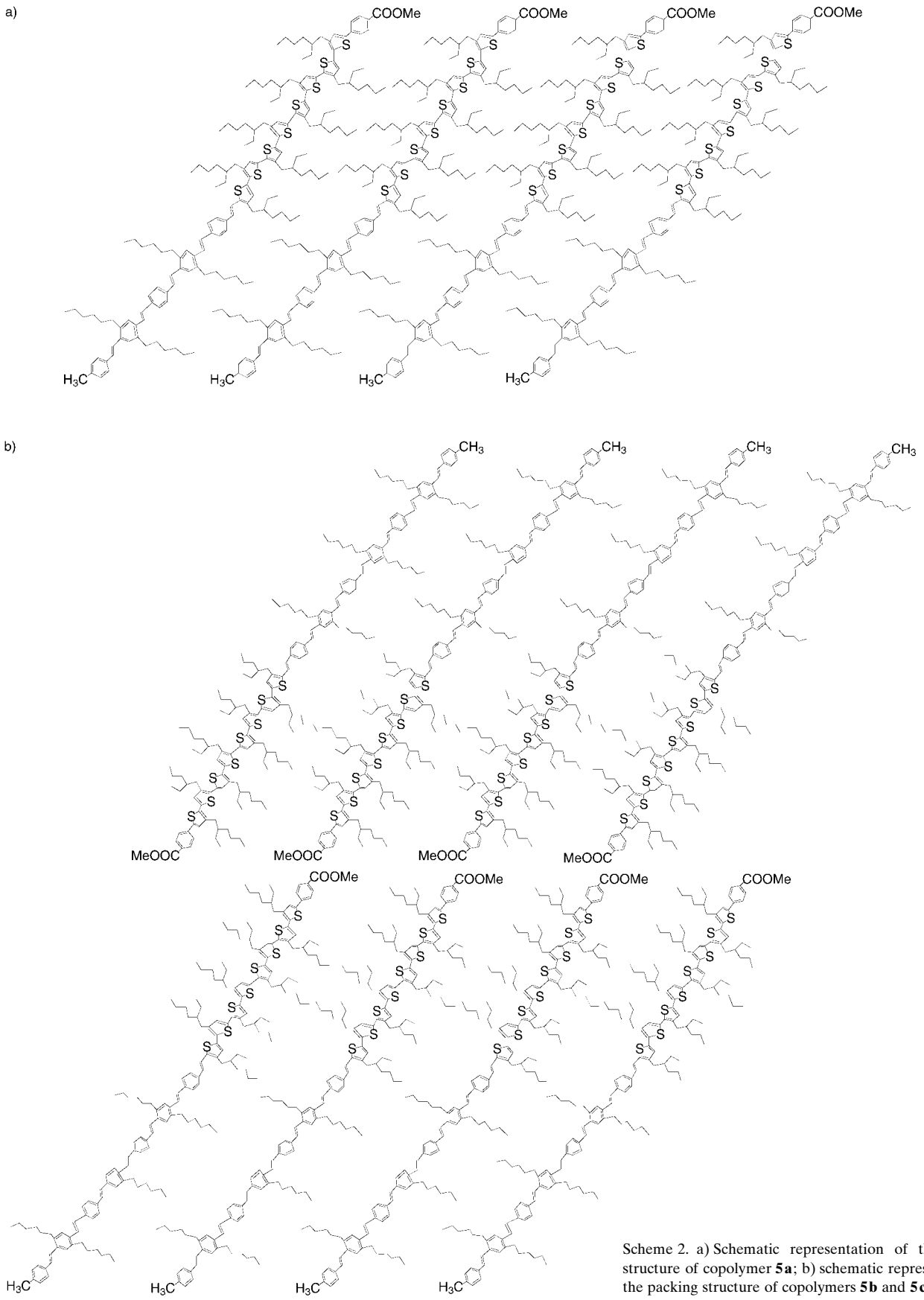

Scheme 2. a) Schematic representation of the packing structure of copolymer **5a**; b) schematic representation of the packing structure of copolymers **5b** and **5c**.

0947-6539/02/0814-3250 $ 20.00+.50/0 *Chem. Eur. J.* **2002**, *8*, No. 14

Table 2. Crystal and structure refinement for compound **6**.[a, b]

empirical formula	$C_{32}H_{41}$
M_w	851.30
T [K]	100
λ [Å]	0.71073
crystal system	triclinic
space group	$P\bar{1}$
unit cell dimensions	
a [Å]	4.8632(10)
α [°]	101.86(3)
b [Å]	12.149(2)
β [°]	91.40(3)
c [Å]	22.149(4)
γ [°]	91.96(3)
V [Å^3]	1279.3(4)
Z	2
ρ_{calcd} [mg m^{-3}]	1.105
μ [mm^{-1}]	0.062
$F(000)$	466
crystal size [mm], color, habit	0.40 × 0.12 × 0.04, yellow, long plate
θ range [°]	1.71–25.03
index ranges	$-5 \le h \le 5$, $-14 \le k \le 10$, $-25 \le l \le 26$
reflections collected	6502
independent reflections	4451 ($R_{int} = 0.0273$)
absorption correction	SADABS based on redundant diffractions
max. and min. transmission	1.0, 0.831
refinement method	full-matrix least squares on F^2
weighting scheme	$w = q[\sigma^2(F_o^2) + (aP)^2 + bP]^{-1}$ where: $P = (F_o^2 + 2F_c^2)/3$, $a = 0.052$, $b = 3.963$, $q = 1$
data/restraints/parameters	4451/0/292
goodness-of-fit on F^2	1.229
final R indices [$I > 2\sigma(I)$]	$R1 = 0.1231$, $wR2 = 0.2448$
R indices (all data)	$R1 = 0.1338$, $wR2 = 0.2501$
largest diff. peak hole [e Å^{-3}]	0.328, −0.256

[a] Equations of interest: $R_{int} = \Sigma |F_o^2 - \langle F_o^2 \rangle| / \Sigma |F_o^2|$
$R1 = \Sigma \| F_o | - | F_c \| / \Sigma | F_o |$
$wR2 = [\Sigma[w(F_o^2 - F_c^2)^2] / \Sigma[w(F_o^2)^2]]^{1/2}$
$GooF = S = [\Sigma[w(F_o^2 - F_c^2)^2] / (n-p)^{1/2}$
where: $w = q/\sigma^2 (F_o^2) + (aP)^2 + bP$; n = number of independent reflections; q, a, b, P as defined in [b]; p = number of parameters refined. [b] All software and sources of scattering factors are contained in the SHELXTL (version 5.1) program library (G. Sheldrick, Bruker Analytical X-ray Systems, Madison, WI).

with its excitation spectrum. When the emission wavelength was chosen to be the maximum emission of compound **6** (480 nm), we see a complete overlap of the absorption spectrum of **6** with the excitation spectrum of **5a**.

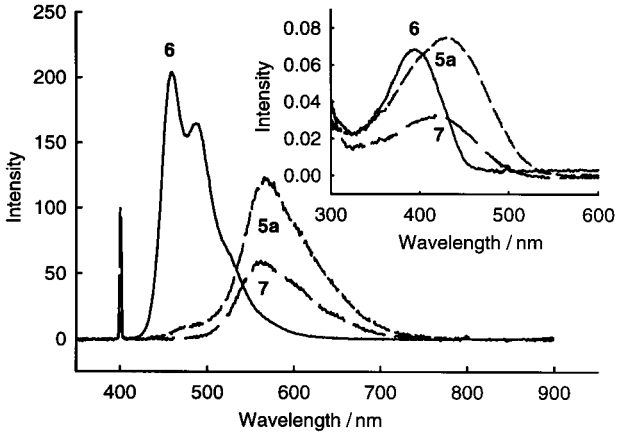

Figure 4. Fluorescence spectra of compounds **6**, **7**, and copolymer **5a** in chloroform (excited at 400 nm). The inset shows the UV/Vis absorption spectra of compounds **6**, **7**, and copolymer **5a** in chloroform.

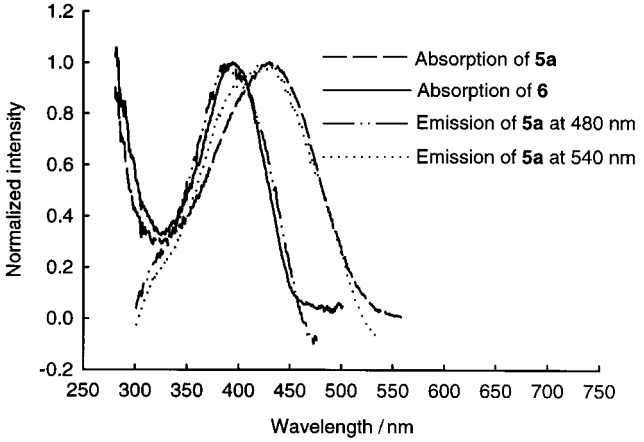

Figure 5. Absorption spectra (copolymer **5a** and compound **6**) and excitation spectra of copolymer **5a** at two different emission wavelengths.

Time-resolved photoluminescence studies were carried out for copolymer **5a** (Figure 6), compound **6**, and **7**. Figure 6 shows a typical result for **5a** and **7**. The fluorescence lifetime

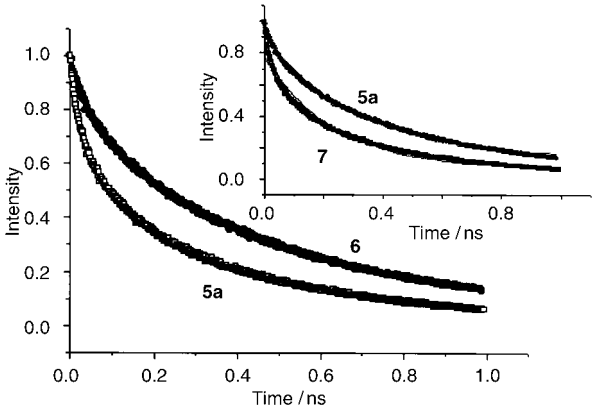

Figure 6. Time-resolved photoluminescence spectra of copolymers **5a**, **6**, and **7**.

was obtained by fitting to a single exponential decay equation: 482 ps for copolymer **5a** and 326 ps for compound **7** (excitation at 390 nm detection at 550 nm). Similar measurements with compound **6** (the excitation at 390 nm and the emission at 480 nm) gave a lifetime of 582 ps. The fluorescence lifetime of the diblock copolymer **5a** is shorter than that of **6** and longer than that of corresponding **7**. The result is consistent with the structural features of diblock copolymers and their associated energy-transfer process. Further studies of ultrafast fluorescence anisotropy revealed a fast decay component (100 fs), which can be attributed to the energy-transfer process.[13]

Conclusion

In summary, we have synthesized a new class of diblock copolymers, rod–rod conjugated diblock copolymers. Interesting intramolecular energy transfer was observed in these

diblock copolymers, and their remarkable self-assembling ability was revealed. These conjugated diblock copolymers are new architectures of electroactive polymers. A great opportunity exists for exploring their electronic and structural properties. Because of the existence of various types of conjugated polymers, it is possible to synthesize diblock copolymers of various combinations of conjugated blocks to give different amphiphilic and electronic properties. These materials will be interesting for studies of photovoltaic effects and molecular electronic components.

Experimental Section

General methods: ^{1}H and ^{13}C NMR spectra were recorded in $CDCl_3$ on a Bruker AM 400 or 500 spectrometer. A Shimadzu DSC-60 differential scanning calorimeter was used to determine the thermal transitions at a heating rate of 10 °C min^{-1}. The results were reported as the maxima and minima of their endothermic or exothermic peaks. A Nikon Optiphoto-2 optical polarized microscope (magnification: ×400) equipped with a Creative devices 50–600 high-temperature stage was used to observe the thermal transitions and to analyze the anisotropic texture. Molecular weight distributions were determined by gel permeation chromatography (GPC) with a Waters Associates liquid chromatograph equipped with a Waters 510 HPLC pump, Waters 410 differential refractometer, and Waters 486 tunable absorbance detector; THF was used as the solvent, and polystyrene as the standard. Elemental analyses were performed by Atlantic Microlab, Inc. MALDI spectra were performed by the University of Illinois at Urbana-Champaign (School of Chemical Sciences, Mass Spectrometry Laboratory). UV/Vis spectra were recorded on a Shimadzu UV-2401PC Recording Spectrophotometer. Emission spectra were recorded on a Shimadzu RF-5301PC Spectrofluorophotometer. The photoluminescence quantum efficiencies were calculated following the procedure in the literature.[9] The compound 9,10-diphenylanthracene was used as the reference.

General materials: 1,4-Dichlorobenzene, 1-bromohexane, methyl 4-methyl benzoate, triethyl phosphite, *N*-bromosuccinimide, 4-methylbenzyl bromide, and the other conventional reagents were used as received. Divinylbenzene was purified according to literature procedure.[8] Tetrahydrofuran was dried by distillation from sodium metal. Ethylene glycol dimethyl ether and *N*,*N*-dimethylformamide were dried by distillation from calcium hydride.

Transmission electron microscopy: As-cast films were prepared by placing a drop of the copolymer solution (0.5 mg ml^{-1}) onto carbon-coated TEM grids. The grids were dried in a solvent atmosphere. The specimen was then examined in a Philips CM120 electron microscope operated at 120 KV.

Small-angle X-ray scattering (SAXS): The synchrotron small-angle X-ray scattering (SAXS) experiment was performed at 15-ID-D beamline of ChemMat CARS at the Advanced Photon Source (APS, Argonne National Labs). The incident X-ray beam produced by a undulator was monochromated and tuned to the energy of 12.398 keV (corresponding to a wavelength of 1.0 Å), using a water-cooled double diamond C(111) crystal, and collimated to 100 μm (500 μm) by a Ta pin-hole. The samples were sandwiched between two Kapton films, then sealed in a furnace. The furnace could heat the sample up to 150 °C. A high-resolution SAXS camera with an image plate was used to collect the scattering images. The distance from the sample to the imaging plate was 1710 mm. The collected two-dimensional images were converted to one-dimensional patterns by a homemade IDL program.

Wide-angle X-ray diffraction (WAXD): The wide-angle X-ray diffraction experiment was performed on a powder diffractometer, which consisted of a Rikagu generator, a Philips wide-angle goniometer, and a digital recording apparatus for X-ray intensities. The generator was generally operated at 40 kV and 20 mA with a Cu tube as the X-ray source. The wide-angle goniometer used a flat-plate sample, and had a graphite monochromator in the receiving position and a scintillation counter for detection. Data collection could range from 2-theta of 4 degrees to about 135 degrees. The goniometer was driven by a stepping motor allowing a minimum step size of 0.002 degrees (2-theta) and any count time at each step. Under computer control any portion of the diffracted spectrum could be recorded for later plotting.

Crystallographic experimental section

Data collection: An irregular broken fragment (0.40 × 0.12 × 0.04 mm) was selected under a stereo-microscope while immersed in Fluorolube oil to avoid possible reaction with air. The crystal was removed from the oil by using a tapered glass fiber that also served to hold the crystal for data collection. The crystal was mounted and centered on a Bruker SMART APEX system at 100 K. Rotation and still images showed the diffractions to be sharp. Frames separated in reciprocal space were obtained and provided an orientation matrix and initial cell parameters. Final cell parameters were obtained from the full data set.

A "hemisphere" data set was obtained, which sampled approximately 1.2 hemispheres of reciprocal space to a resolution of 0.84 Å by using 0.3° steps in ω with 100-second integration times for each frame. Data collection was made at 100 K. Integration of intensities and refinement of cell parameters were done using SAINT [1]. Absorption corrections were applied using SADABS [1] based on redundant diffractions.

Structure solution and refinement: The space group was determined as $P\bar{1}$ based on systematic absences and intensity statistics. Direct methods were used to locate most C atoms from the E-map. Repeated difference Fourier maps allowed recognition of all expected C atoms. Following anisotropic refinement of C atoms, H atom positions were calculated. Final refinement was anisotropic for C atoms and isotropic for H atoms. No anomalous bond lengths or thermal parameters were noted. All ORTEP diagrams have been drawn with 50% probability ellipsoids.

Synthesis: A general synthetic procedure is outlined in Scheme 1. The synthesis of compounds **1**, **2**, and **4** has been described previously.[7, 10, 11]

Compound 3: Compound **1b** (1.314 g, 0.76 mmol) and compound **2** (0.57 g, 0.99 mmol) were dissolved in anhydrous 1,2-dimethoxyethane (20 mL), and then NaH (1.5 equiv) was added. The resulting solution was stirred under reflux for 2 hours, then cooled to 0 °C, and poured into water (100 mL). A small amount of acetic acid was added to neutralize the excess amount of base. The solution was extracted with chloroform three times, and then the combined organic layer was dried over Na_2SO_4. The solvent was removed by rotary evaporation, and the residue was purified by flash chromatography (silica gel (300 mesh), hexane/ethyl acetate (50:1)) to give the pure product (84% yield).

^{1}H NMR (400 MHz, $CDCl_3$, 25 °C, TMS): δ = 8.04 (d, J = 8.4 Hz, 2H), 7.65 (d, J = 8.4 Hz, 2H), 7.48 (dd, J_1 = 11.9 Hz, J_2 = 8.1 Hz, 4H), 7.43 (s, 1H), 7.34 (s, 1H), 7.27 (d, J = 16.0 Hz, 2H), 7.23 (s, 1H), 6.98 (d, J = 16.1 Hz, 1H), 6.97 (s, 1H), 6.94 (s, 5H), 6.89 (s, 1H), 6.86 (d, J = 15.9 Hz, 1H), 3.93 (s, 3H), 2.71 (m, 11H), 2.62 (d, J = 7.0 Hz, 1H), 1.75 (m, 8H), 1.63 (m, 4H), 1.31 (m, 76H), 0.89 (m, 54H); ^{13}C NMR (500 MHz, $CDCl_3$, 25 °C, TMS): δ = 10.71, 10.93, 14.02, 14.06, 14.11, 22.54, 22.58, 23.01, 23.06, 25.73, 28.69, 28.73, 28.90, 29.11, 30.08, 31.59, 31.63, 32.58, 32.66, 33.57, 35.87, 40.09, 40.15, 41.03, 52.04, 120.00, 123.35, 124.98, 125.15, 126.45, 126.84, 127.06, 128.04, 128.57, 128.96, 129.43, 129.50, 129.65, 129.74, 130.20, 131.00, 131.14, 131.37, 132.30, 133.22, 133.37, 133.50, 133.54, 134.96, 136.56, 136.80, 138.26, 138.99, 139.60, 139.93, 141.02, 166.65; MS: m/z: 2141.71 [M^+]; elemental analysis calcd (%) for $C_{132}H_{187}BrO_2S_8$ (2142.2): C 74.00, H 8.80, Br 3.73, S 11.97; found: C 74.14, H 8.91, Br 3.62, S 11.89.

Compound 5a (n = 2): Compound **3** (389 mg, 0.18 mmol), tri-*o*-tolylphosphine (10.9 mg, 0.036 mmol), NBu_3 (0.036 mL, 0.2 mmol), [$Pd(OAc)_2$] (2.0 mg, 0.009 mmol), and compound **4a** (97.4 mg, 0.20 mmol) were dissolved in anhydrous DMF (*N*,*N*-dimethylformamide, 5 mL). The mixture was stirred at 110 °C for 24 hours and then cooled to room temperature, and poured into methanol (50 mL). The precipitate was collected by suction filtration and washed with excess methanol. The product was purified by column chromatography using a mixture of ethyl acetate and hexane as the eluent to give pure **5a** as a dark red solid (56% yield).

^{1}H NMR (400 MHz, $CDCl_3$, 25 °C, TMS): δ = 8.04 (d, J = 8.6 Hz, 2H), 7.65 (d, J = 8.6 Hz, 2H), 7.54 (s, 4H), 7.51–7.42 (m, 1H), 7.39 (d, J = 16.2 Hz, 3H), 7.31 (d, J = 16.0 Hz, 2H), 7.23 (s, 1H), 7.19 (d, J = 8.1 Hz, 2H), 7.06 (d, J = 16.1 Hz, 1H), 7.04 (d, J = 16.1 Hz, 2H), 7.02 (d, J = 16.2 Hz, 1H), 6.98 (s, 1H), 6.95 (s, 5H), 6.90 (s, 1H), 6.87 (d, J = 15.9 Hz, 1H), 3.93 (s, 3H), 2.74 (m, 22H), 2.63 (d, J = 6.6 Hz, 2H), 2.38 (s, 3H), 1.70 (m, 16H), 1.34 (m, 88H), 0.90 (m, 60H); ^{13}C NMR (500 MHz, $CDCl_3$, 25 °C, TMS): δ = 10.74, 10.96, 14.10, 14.14, 21.21, 22.64, 23.05, 23.09, 25.71, 25.76, 28.71, 28.75, 28.93,

  0947-6539/02/0814-3252 $ 20.00+.50/0 *Chem. Eur. J.* **2002**, *8*, No. 14

29.34, 29.67, 31.34, 31.41, 31.71, 32.60, 33.29, 33.60, 33.71, 40.11, 40.18, 41.06, 52.05, 119.88, 125.00, 125.77, 125.86, 126.37, 126.47, 126.54, 126.59, 126.80, 126.92, 128.07, 128.58, 128.75, 128.89, 128.98, 129.27, 129.36, 129.46, 129.53, 129.76, 130.22, 131.04, 131.07, 131.17, 131.39, 131.46, 132.32, 133.17, 133.42, 133.52, 133.56, 134.70, 134.94, 135.05, 135.16, 136.65, 136.93, 136.97, 137.04, 137.13, 137.31, 138.27, 138.41, 138.51, 138.56, 139.01, 139.94, 139.98, 140.97, 166.67; MS: m/z: 2551.57 [M^+]; elemental analysis calcd (%) for $C_{169}H_{232}O_2S_8$ (2552.2): C 79.53, H 9.16, S 10.05; found: C 79.34, H 9.10, S 9.94.

Compound 5b ($n = 3$): Refer to the experimental procedure of compound **5a** (55% yield).

^{1}H NMR (400 MHz, $CDCl_3$, 25 °C, TMS): $\delta = 8.05$ (d, $J = 8.5$ Hz, 2H), 7.65 (d, $J = 8.5$ Hz, 2H), 7.54 (m, 8H), 7.51–7.42 (m, 12H), 7.41–7.37 (m, 5H), 7.31 (d, $J = 16.0$ Hz, 2H), 7.23 (s, 1H), 7.19 (d, $J = 8.2$ Hz, 2H), 7.06 (d, $J = 16.2$ Hz, 3H), 7.05 (d, $J = 16.0$ Hz, 2H), 7.02 (d, $J = 16.4$ Hz, 1H), 6.98 (s, 1H), 6.95 (s, 5H), 6.90 (s, 1H), 6.87 (d, $J = 15.9$ Hz, 1H), 3.93 (s, 3H), 2.75 (m, 26H), 2.64 (d, $J = 6.4$ Hz, 2H), 2.38 (s, 3H), 1.70 (m, 20H), 1.37–1.29 (m, 100H), 0.90 (m, 66H); ^{13}C NMR (500 MHz, $CDCl_3$, 25 °C, TMS): $\delta =$ 10.73, 10.94, 14.08, 14.12, 14.30, 22.62, 23.03, 23.07, 25.69, 25.74, 28.69, 28.74, 28.92, 29.32, 29.65, 31.32, 31.39, 31.69, 32.54, 32.58, 33.28, 33.58, 33.66, 33.69, 40.10, 40.16, 52.05, 119.88, 124.96, 125.01, 125.80, 125.86, 126.36, 126.46, 126.53, 126.59, 126.79, 126.90, 127.50, 128.01, 128.06, 128.58, 128.75, 128.88, 128.97, 129.26, 129.35, 129.44, 129.52, 129.74, 130.17, 130.21, 131.02, 131.05, 131.15, 131.36, 131.43, 132.24, 132.30, 133.16, 133.40, 133.55, 134.69, 134.93, 135.04, 135.16, 136.64, 136.91, 137.06, 137.31, 138.16, 138.27, 138.40, 138.51, 138.56, 139.00, 139.94, 140.05, 140.96, 166.66; MS: m/z: 2923.99 [M^+]; elemental analysis calcd (%) for $C_{197}H_{266}O_2S_8$ (2922.8): C 80.95, H 9.26, S 8.73; found: C 80.76, H 9.33, S 8.47.

Compound 5c ($n = 4$): Refer to the experimental procedure of compound **5a** (60% yield).

^{1}H NMR (400 MHz, $CDCl_3$, 25 °C, TMS): $\delta = 8.03$ (d, $J = 8.3$ Hz, 2H), 7.64 (d, $J = 8.3$ Hz, 2H), 7.53–7.36 (m, 33H), 7.30 (d, $J = 16.0$ Hz, 2H), 7.22 (s, 1H), 7.17 (d, $J = 8.2$ Hz, 2H), 7.07–6.98 (m, 8H), 6.97 (s, 1H), 6.94 (s, 5H), 6.89 (s, 1H), 6.86 (d, $J = 15.9$ Hz, 1H), 3.92 (s, 3H), 2.74 (m, 32H), 2.63 (d, $J = 6.5$ Hz, 2H), 2.36 (s, 3H), 1.65 (m, 24H), 1.53–1.29 (m, 112H), 0.90 (m, 72H); ^{13}C NMR (500 MHz, $CDCl_3$, 25 °C, TMS): $\delta = 10.73$, 10.95, 14.09, 14.13, 14.30, 21.21, 22.63, 23.04, 23.08, 25.75, 28.69, 28.74, 28.92, 29.33, 29.65, 31.33, 31.40, 31.70, 32.59, 33.29, 33.58, 33.66, 33.70, 40.17, 41.04, 52.06, 119.88, 124.96, 125.00, 125.79, 125.85, 126.36, 126.47, 126.53, 126.59, 126.80, 128.02, 128.74, 128.88, 129.26, 129.35, 129.44, 129.52, 129.74, 130.17, 130.21, 131.03, 131.15, 131.37, 131.43, 132.25, 133.16, 133.41, 133.51, 134.69, 134.93, 135.04, 135.15, 136.63, 136.92, 137.08, 137.31, 138.41, 138.51, 138.56, 139.01, 139.94, 140.05, 140.96, 166.22; MS: m/z: 3299.55 [M^+]; elemental analysis calcd (%) for $C_{225}H_{304}O_2S_8$ (3297.4): C 82.00, H 9.29, S 7.78; found: C 81.78, H 9.21, S 7.49.

Acknowledgments

This work was supported by US NSF and AFOSR (L.P.Y.). This work also benefited from the support of the NSF MERSEC program at the University of Chicago. We thank Dr. David Cookson, Dr. Tadanori, and Dr. P. James Viccaro for their assistance in SAXS/WAXS data collection and analysis. We also thank Professor Ted Goodson for his assistance in Ultra-fast spectroscopy. ChemMatCARS Sector 15 is principally supported by the National Science Foundation/Department of Energy under grant numbers CHE9522232 and CHE0087817 and by the Illinois board of higher education. The Advanced Photon Source is supported by the U.S. Department of Energy, Basic Energy Sciences, and the Office of Science under Contract No. W-31-109-Eng-38.

[1] *Handbook of Conducting Polymers*, 2nd ed. (Eds.: T. A. Skotheim, R. L. Elsenbaumer, J. R. Reynolds), Marcel Dekker, New York, **1998**.
[2] *Handbook of Organic Conductive Molecules and Polymers*, *Vols. 1–4* (Ed.: H. S. Nalwa), **1997**.
[3] *Electroresponsive Molecular and Polymeric Systems*, *Vols. 1–2* (Ed.: T. A. Skotheim), Marcel Dekker, New York, **1991**.
[4] a) N. C. Greenham, S. C. Moratti, D. D. C. Bradley, R. H. Friend, A. B. Holmes, *Nature* **1993**, *365*, 628–630; b) D. Braun, A. J. Heeger, *Appl. Phys. Lett.* **1991**, *58*, 1982–1984; c) F. Hide, M. A. Diazgarcia, B. J. Schwartz, M. R. Anderson, Q. B. Pei, A. J. Heeger, *Science* **1996**, *273*, 1833–1836.
[5] W. J. Li, L. P. Yu, *Macromolecules* **1996**, *29*, 7329–7334.
[6] W. J. Li, H. B. Wang, L. P. Yu, T. L. Morkved, H. M. Jaeger, *Macromolecules* **1999**, *32*, 3034–3044.
[7] H. B. Wang, H. Wang, V. S. Urban, P. Thiyagarajan, K. C. Littrell, L. P. Yu, *J. Am. Chem. Soc.* **2000**, *122*, 6855–6861.
[8] B. T. Strey, *J. Polym. Sci. Part A* **1965**, *3*, 265–282.
[9] J. N. Demas, G. A. Crosby, *J. Phys. Chem.* **1971**, *75*, 991–1024.
[10] T. M. Maddux, W. J. Li, L. P. Yu, *J. Am. Chem. Soc.* **1997**, *119*, 844–845.
[11] M.-K. Ng, L. M. Wang, L. P. Yu, *Chem. Mater.* **2000**, *12*, 2988–2995.
[12] D. W. Van Krevelen, *Properties of Polymers: Their Estimation and Correlation with Chemical Structure*, Elsevier, New York, **1976**, p. 129–130.
[13] S. Lahahkar, H. B. Wang, L. P. Yu, T. Goodson III, unpublished results.

Received: December 20, 2001 [F3753]